The 2009 IEEE/RSJ International Conference on
Intelligent Robots and Systems
October 11-15, 2009 St. Louis, USA

Adaptive Control for a Torque Controlled Free-Floating Space Robot with Kinematic and Dynamic Model Uncertainty

Satoko Abiko* and Gerd Hirzinger**
*Department of Aerospace Engineering, Tohoku University
Aramaki-Aza Aoba 6-6-01, Sendai, Japan
**Institute of Robotics and Mechatronics
German Aerospace Center (DLR)
D-82334, Weßling, Germany
satoko.abiko@ieee.org

***Abstract*— This paper proposes an adaptive controller for a fully free-floating space robot with kinematic and dynamic model uncertainty. In adaptive control design for the space robot, because of high dynamical coupling between an actively operated arm and a passively moving end-point, two inherent difficulties exist, such as non-linear parameterization of the dynamic equation and both kinematic and dynamic parameter uncertainties in the coordinate mapping from Cartesian space to joint space. The proposed method in this study overcomes the above two issues by paying attention to the coupling dynamics. The proposed adaptive controller does not involve any measurement of acceleration; but it is still possible for the system to be linearly parameterized in terms of uncertain parameters and a suitable input torque can be generated in the presence of model uncertainty. A numerical simulation was carried out to confirm the validity of the proposed adaptive control.**

***Index Terms*— Adaptive Control, Model Uncertainty, Inverted Chain Approach, Free-Floating Space Robot**

I. INTRODUCTION

Robotics technology has been recently exploited in a variety of areas and various types of robots have been developed to accomplish sophisticated tasks in different fields. On-orbit servicing robots are examples of outer space applications. The space robots are expected to achieve various tasks, such as capturing a target, constructing a large structure and autonomously maintaining on-orbit systems. In these missions, one fundamental task with the robotic system would be the tracking, the grasping and the positioning of a target in Cartesian space. This paper addresses the task of following a desired trajectory in Cartesian space while the space robot grasps a target whose dynamic properties are unknown. The model uncertainty causes a tracking problem, where a given nominal trajectory has to be tracked, while accounting for the parameter uncertainty.

To cope with such an issue, this paper proposes an adaptive control of a free-floating space robot. In free-floating space robots, because of high dynamical coupling between a passively moving part in Cartesian space (end-point) and an actively operated robot arm, two unique issues exist in the control design in the presence of model uncertainty. Firstly, the end-point of the robot arm is governed by the coordinate mapping from Cartesian space to joint space, which is strongly subject to the uncertainty of both kinematic and dynamic properties. Secondly, the dynamic equation is not simply linearly parameterized in terms of uncertain parameters because of the nature of the coupling dynamics. These two problems induce the difficulty in adaptive control design of space robots.

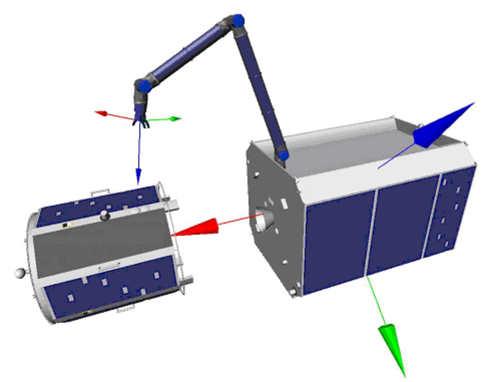

Fig. 1: Chaser-robot and target scenario

In fixed-based manipulator systems, Slotine and Li proposed adaptive controllers to track a given trajectory in both joint and Cartesian space while compensating for the dynamic parameter uncertainty of a grasped target in [1] [2]. Xu *et al.* [3] used the same approach of adaptive controller design as proposed in [1] for the space robot on the assumption that the base satellite attitude is perfectly controlled. However, it is practically impossible to perfectly control the base attitude because of the poor performance of attitude control devices, (*e.g.* thrusters and reaction wheels) and time delay in feedback controllers. Gu and Xu [4] introduced another adaptive control for fully floating space robot; however, for the implementation of this method, it is essential to measure the linear and angular accelerations of the base satellite, which is again difficult because the acceleration measurement is susceptive to sensor noise and drift in practice. Wee *et al.* [5] proposed an adaptive control method with parameter identification based on the principle of conservation of momentum. However, the proposed method does not explicitly solve the nonlinear parameterization problem associated with the computed torque control for the free-floating space robots. Abiko and Hirzinger [6] developed an alternative adaptive controller by using a velocity-based closed-loop controller for generating a torque input. Using this control input, one does not encounter the nonlinear parameterization problem, but tuning gain parameters for the torque input is still a key issue and explicit description of the torque input in the adaptive control method is desired.

Cheah *et al.* [7] introduced an adaptive Jacobian tracking control for a fixed-based manipulator system with kinematic, dynamic, and actuator model uncertainties. The proposed method in [7] designed an adaptation law for kinematic parameters with kinematic mapping and another adaptation law for dynamic parameters with dynamic equation, separately. However, this approach is not simply applicable to the space robot since there exists major difference between the fixed-based manipulator system and the space robot, *i.e.* the space robot exhibits high dynamical coupling because its base satellite is inertially free. As mentioned previously, dynamical coupling causes the complexity of the coordinate mapping and the difficulty of the linearized parameterization in the dynamic equation in the free-floating space robot, while the kinematic and dynamic parameter errors can be exclusively handled in the fixed-based manipulator system.

This paper proposes an adaptive controller for a torque-controlled *fully* free-floating space robot with both kinematic and dynamic model uncertainty. A novel feature of the proposed method is that it does not involve the measurment of the acceleration of the system; however, it is still possible for the system to be linearly parameterized in terms of uncertain parameters. The paper is organized as follows. Section II describes the dynamic model and properties of the free-floating space robot. Section III introduces operational space trajectory tracking control based on passivity theorem and proposes an adaptive controller for the fully free-floating space robot. Section IV gives details about numerical simulation of the proposed mothod using a realistic three-dimensional model. Section V summarizes the conclusions.

II. MODELING OF FREE-FLOATING SPACE ROBOT

In the conventional dynamic expressions, linear and angular velocities of the base satellite and the motion rate of each joint are selected as the generalized coordinates [8]. However, due to the lack of a fixed base, the space robot can be expressed by the motion of the end effector and that of the robotic joints in the same structure as in the conventional expression. This scheme is termed *inverted chain approach* [6].

The following subsections explain the dynamic equations of the system in inverted chain approach, for a serial rigid-link manipulator attached to a floating base, as shown in Fig. 2. The main notations used in this section are listed in Table I.

A. Equations of motion

Let us consider the linear and angular velocities of the end-effector, $\dot{\boldsymbol{x}}_e = (\boldsymbol{v}_e^T, \boldsymbol{\omega}_e^T)^T \in R^{6\times1}$ and the motion rate

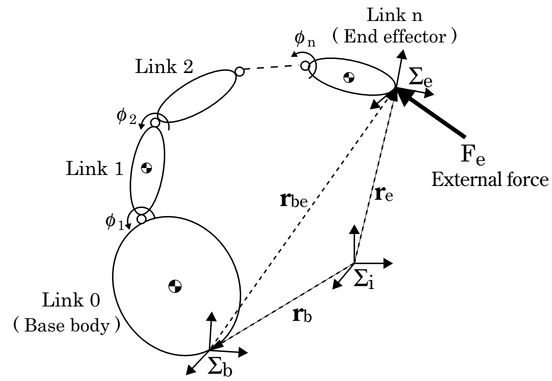

Fig. 2: General model of space robot

of the joints, $\dot{\boldsymbol{\phi}} \in R^{n\times1}$ as the generalized coordinates The equations of motion are expressed in the following form:

$$\begin{bmatrix} \boldsymbol{H}_e & \boldsymbol{H}_{em} \\ \boldsymbol{H}_{em}^T & \boldsymbol{H}_m \end{bmatrix} \begin{bmatrix} \ddot{\boldsymbol{x}}_e \\ \ddot{\boldsymbol{\phi}} \end{bmatrix} + \begin{bmatrix} \boldsymbol{c}_e & \boldsymbol{c}_{em} \\ \boldsymbol{c}_{em}^T & \boldsymbol{c}_m \end{bmatrix} \begin{bmatrix} \dot{\boldsymbol{x}}_e \\ \dot{\boldsymbol{\phi}} \end{bmatrix} = \begin{bmatrix} \mathcal{F}_e \\ \boldsymbol{\tau} \end{bmatrix} + \begin{bmatrix} \boldsymbol{J}_e^T \\ \boldsymbol{J}_m^T \end{bmatrix} \mathcal{F}_b. \quad (1)$$

The upper part of eq. (1) describes the coordinate mapping for the free-floating robot in acceleration level, where both kinematic and dynamic parameters exist. The lower part of eq. (1) expresses the dynamic equation in joint space including the dynamical coupling motion of the end-effector.

Property 1: The equation (1) can be linearized in terms of certain parameters:

$$\boldsymbol{H}_e\ddot{\boldsymbol{x}}_e + \boldsymbol{H}_{em}\ddot{\boldsymbol{\phi}} + \boldsymbol{c}_e\dot{\boldsymbol{x}}_e + \boldsymbol{c}_{em}\dot{\boldsymbol{\phi}} = \boldsymbol{Z}\boldsymbol{a}\ , \quad (2)$$

$$\boldsymbol{H}_{em}^T\ddot{\boldsymbol{x}}_e + \boldsymbol{H}_m\ddot{\boldsymbol{\phi}} + \boldsymbol{c}_{em}^T\dot{\boldsymbol{x}}_e + \boldsymbol{c}_m\dot{\boldsymbol{\phi}} = \boldsymbol{Y}\boldsymbol{a}\ , \quad (3)$$

where $\boldsymbol{a}$ is a vector with suitable kinematic and dynamic parameters. $\boldsymbol{Z} = \boldsymbol{Z}(\boldsymbol{x}_e, \dot{\boldsymbol{x}}_e, \ddot{\boldsymbol{x}}_e, \boldsymbol{\phi}, \dot{\boldsymbol{\phi}}, \ddot{\boldsymbol{\phi}})$ and $\boldsymbol{Y} = \boldsymbol{Y}(\boldsymbol{x}_e, \dot{\boldsymbol{x}}_e, \ddot{\boldsymbol{x}}_e, \boldsymbol{\phi}, \dot{\boldsymbol{\phi}}, \ddot{\boldsymbol{\phi}})$ are known as regressor matrices and functions of state values.

Property 2: The inertia matrices $\boldsymbol{H}_e \in R^{6\times6}$, $\boldsymbol{H}_m \in R^{n\times n}$ and $\boldsymbol{H} = \begin{bmatrix} \boldsymbol{H}_e & \boldsymbol{H}_{em} \\ \boldsymbol{H}_{em}^T & \boldsymbol{H}_m \end{bmatrix} \in R^{(6+n)\times(6+n)}$ are symmetric and uniformly positive definite for all $\boldsymbol{x}_e \in R^{6\times1}$ and $\boldsymbol{\phi} \in R^{n\times1}$.

Property 3: The following matrices are skew symmetric:

$$\boldsymbol{S}_e = \boldsymbol{c}_e - \frac{1}{2}\dot{\boldsymbol{H}}_e, \quad \boldsymbol{S}_m = \boldsymbol{c}_m - \frac{1}{2}\dot{\boldsymbol{H}}_m, \quad \boldsymbol{S} = \boldsymbol{c} - \frac{1}{2}\dot{\boldsymbol{H}},$$

such that:

$$\boldsymbol{\nu}_e^T\boldsymbol{S}_e\boldsymbol{\nu}_e = 0,\ \boldsymbol{\nu}_m^T\boldsymbol{S}_m\boldsymbol{\nu}_m = 0,\ \boldsymbol{\nu}^T\boldsymbol{S}\boldsymbol{\nu} = 0,$$

for all $\boldsymbol{\nu}_e \in R^{6\times1}$, $\boldsymbol{\nu}_m \in R^{n\times1}$, and $\boldsymbol{\nu} \in R^{(6+n)\times1}$, respectively. $\boldsymbol{c} = \begin{bmatrix} \boldsymbol{c}_e & \boldsymbol{c}_{em} \\ \boldsymbol{c}_{em}^T & \boldsymbol{c}_m \end{bmatrix} \in R^{(6+n)\times(6+n)}$.

B. Momentum equation

The integral of the upper part of eq. (1) represents total linear and angular momentum of the system around the end-effector:

$$\mathcal{L}_e = \boldsymbol{H}_e\dot{\boldsymbol{x}}_e + \boldsymbol{H}_{em}\dot{\boldsymbol{\phi}}. \quad (4)$$

TABLE I: Main notations in dynamic equations

n		: number of joints.
$\boldsymbol{v}_e$	$\in R^{3\times 1}$	: linear velocity of the end-effector.
$\boldsymbol{\omega}_e$	$\in R^{3\times 1}$	: angular velocity of the end-effector.
$\dot{\boldsymbol{x}}_e$	$\in R^{6\times 1}$	: spatial velocity of the end-effector.
$\boldsymbol{\phi}$	$\in R^{n\times 1}$	: vector for the joint angle of the arm.
$\boldsymbol{H}_e$	$\in R^{6\times 6}$	: inertia matrix of the end-effector.
$\boldsymbol{H}_m$	$\in R^{n\times n}$	: inertia matrix of the robot arm.
$\boldsymbol{H}_{em}$	$\in R^{6\times n}$	: coupling inertia matrix between the end-effector and the arm.
$\boldsymbol{c}_e$	$\in R^{6\times 6}$	: non-linear velocity dependent term on the end-effector.
$\boldsymbol{c}_m$	$\in R^{n\times n}$	: non-linear velocity dependent term of the arm.
$\boldsymbol{c}_{em}$	$\in R^{6\times n}$	: coupling non-linear velocity dependent term between the end-effector and the arm.
$\mathcal{F}_e$	$\in R^{6\times 1}$	: force and moment exerted on the end-effector.
$\mathcal{F}_b$	$\in R^{6\times 1}$	: force and moment exerted on the base.
$\boldsymbol{\tau}$	$\in R^{n\times 1}$	: torque on joints.
$\mathcal{L}_e$	$\in R^{6\times 1}$	: total linear and angular momentum around the end-effector.
$\boldsymbol{J}_e$	$\in R^{6\times 6}$	: Jacobian matrix related to the end-effector and the base.
$\boldsymbol{J}_m$	$\in R^{6\times n}$	: Jacobian matrix related to the arm and the base.

The above equation governs the motion of the free-floating space robot. Therefore, the coordinate mapping in velocity level is expressed as follows:

$$\dot{\boldsymbol{x}}_e = \boldsymbol{J}_e^* \dot{\boldsymbol{\phi}} + \boldsymbol{H}_e^{-1}\mathcal{L}_e, \tag{5}$$

where $\boldsymbol{J}_e^* = -\boldsymbol{H}_e^{-1}\boldsymbol{H}_{em} \in R^{6\times n}$ represents the generalized Jacobian matrix for the end-effector.

C. Dynamics in joint space

The dynamic equation for the free-floating space robot is reduced a form expressed by only joint acceleration, $\ddot{\boldsymbol{\phi}}$, by eliminating the end-effector acceleration, $\ddot{\boldsymbol{x}}_e$ from eq. (1) as follows:

$$\boldsymbol{H}^*\ddot{\boldsymbol{\phi}} + \boldsymbol{c}^* = \boldsymbol{\tau} + \boldsymbol{J}_e^{*T}\mathcal{F}_e + \boldsymbol{J}_b^{*T}\mathcal{F}_b, \tag{6}$$

where

$$\boldsymbol{H}^* = \boldsymbol{H}_m - \boldsymbol{H}_{em}^T\boldsymbol{H}_e^{-1}\boldsymbol{H}_{em} \in R^{n\times n},$$

$$\boldsymbol{J}_b^* = \boldsymbol{J}_m - \boldsymbol{J}_e\boldsymbol{H}_e^{-1}\boldsymbol{H}_{em} \in R^{6\times n}.$$

The inertia matrix $\boldsymbol{H}^*$ is symmetric positive definite. The Jacobian matrix $\boldsymbol{J}_b^*$ represents the generalized Jacobian matrix in terms of the base satellite. The vector $\boldsymbol{c}^* \in R^{n\times 1}$ represents the non-linear velocity dependent term expressed as follows:

$$\boldsymbol{c}^* = \left(\boldsymbol{c}_m - \boldsymbol{H}_{em}^T\boldsymbol{H}_e^{-1}\boldsymbol{c}_{em}\right)\dot{\boldsymbol{\phi}} + \left(\boldsymbol{c}_{em}^T - \boldsymbol{H}_{em}^T\boldsymbol{H}_e^{-1}\boldsymbol{c}_e\right)\dot{\boldsymbol{x}}_e. \tag{7}$$

The above vector can be described by a reduced form expressed by only the joint motion using eq. (5). Then, $\boldsymbol{c}^*$ possesses the following notable property.

Property 4: On the assumption of zero total linear and angular momentum ($\mathcal{L}_e = \mathbf{0}$), the non-linear velocity dependent term, $\boldsymbol{c}^*$, can be expressed in the linearized form in terms of the joint velocity [9]:

$$\boldsymbol{c}^* = \dot{\boldsymbol{H}}^*\dot{\boldsymbol{\phi}} - \frac{\partial}{\partial\boldsymbol{\phi}}\left(\frac{1}{2}\dot{\boldsymbol{\phi}}^T\boldsymbol{H}^*\dot{\boldsymbol{\phi}}\right) = \boldsymbol{c}_m^*\dot{\boldsymbol{\phi}}\ . \tag{8}$$

Equation (8) has the following feature; the matrix $\boldsymbol{S}^* = \boldsymbol{c}_m^* - \frac{1}{2}\dot{\boldsymbol{H}}^*$ is skew symmetric, such that $\boldsymbol{\nu}_m^T\boldsymbol{S}^*\boldsymbol{\nu}_m = 0$ for all $\boldsymbol{\nu}_m \in R^{n\times 1}$.

III. ADAPTIVE CONTROL FOR TRAJECTORY TRACKING CONTROL

A. Adaptive Controller Design

The presence of dynamic parameter errors degrades the control performance of the above method and, in the worst case, causes instability in the closed-loop. This section proposes an adaptive control technique to compensate for the model uncertainties in the trajectory tracking control in Cartesian space for the space robot.

Let us define a reference output velocity $\boldsymbol{\eta}$ and a reference output acceleration $\dot{\boldsymbol{\eta}}$ as follows:

$$\begin{aligned}\boldsymbol{\eta} &= \dot{\boldsymbol{x}}_e^d + \boldsymbol{K}_v\widetilde{\boldsymbol{x}}_e,\\ \dot{\boldsymbol{\eta}} &= \ddot{\boldsymbol{x}}_e^d + \boldsymbol{K}_v\dot{\widetilde{\boldsymbol{x}}}_e.\end{aligned} \tag{9}$$

The reference error $\boldsymbol{s}$ between the reference output $\boldsymbol{\eta}$ and the actual velocity $\dot{\boldsymbol{x}}_e$ is defined as:

$$\boldsymbol{s} = \boldsymbol{\eta} - \dot{\boldsymbol{x}}_e = \dot{\widetilde{\boldsymbol{x}}}_e + \boldsymbol{K}_v\widetilde{\boldsymbol{x}}_e. \tag{10}$$

In the above equations, $\boldsymbol{K}_v \in R^{6\times 6}$ is a strictly positive definite matrix. $\dot{\boldsymbol{x}}_e^d = \left(\boldsymbol{v}_e^{dT}, \boldsymbol{\omega}_e^{dT}\right)^T \in R^{6\times 1}$ represents the desired velocity of the end-effector. $\widetilde{\boldsymbol{x}}_e = \left(\boldsymbol{e}_p^T, \boldsymbol{e}_o^T\right)^T \in R^{6\times 1}$ represents the operational space error consisting of the position error $\boldsymbol{e}_p \in R^{3\times 1}$ and the orientation error $\boldsymbol{e}_o \in R^{3\times 1}$. The position error $\boldsymbol{e}_p$ is simply expressed as follows:

$$\boldsymbol{e}_p = \boldsymbol{r}_e^d - \boldsymbol{r}_e.$$

The orientation error $\boldsymbol{e}_o$ is expressed in terms of the quaternion expression $\mathcal{Q} = \left[\xi, \boldsymbol{\epsilon}^T\right]$ where ξ and $\boldsymbol{\epsilon}$ represent the scalar and vector parts of the quaternion as follows:

$$\boldsymbol{e}_o = \Delta\boldsymbol{\epsilon} = \xi\boldsymbol{\epsilon}^d - \xi^d\boldsymbol{\epsilon} - \boldsymbol{\epsilon}^d \times \boldsymbol{\epsilon},$$

where the operator $\times$ denotes the cross-product operator.

By using the above preliminary information, the following trajectory tracking control with model uncertainties and an adaptive control are determined:

1) joint space reference acceleration and velocity:

$$\begin{aligned}\ddot{\boldsymbol{\phi}}^r &= -\widehat{\boldsymbol{H}}_{em}^+(\widehat{\boldsymbol{H}}_e\dot{\boldsymbol{\eta}} + \widehat{\boldsymbol{c}}_e\boldsymbol{\eta} + \widehat{\boldsymbol{c}}_{em}\dot{\boldsymbol{\phi}} + \boldsymbol{\Lambda}\boldsymbol{s}),\\ \dot{\boldsymbol{\phi}}^r &= -\widehat{\boldsymbol{H}}_{em}^+\widehat{\boldsymbol{H}}_e\boldsymbol{\eta},\end{aligned} \tag{11}$$

2) input torque:

$$\boldsymbol{\tau} = \widehat{\boldsymbol{H}}_{em}^T \dot{\boldsymbol{\eta}} + \widehat{\boldsymbol{H}}_m \ddot{\boldsymbol{\phi}}^r + \widehat{\boldsymbol{c}}_{em}^T \boldsymbol{\eta} + \widehat{\boldsymbol{c}}_m \dot{\boldsymbol{\phi}}^r + \boldsymbol{\Lambda}_q \boldsymbol{s}_q, \quad (12)$$

3) adaptive control law:

$$\dot{\widehat{\boldsymbol{a}}} = -\boldsymbol{\Gamma}^{-1}\big(\boldsymbol{Y}^T \boldsymbol{s} + \boldsymbol{Z}^T \boldsymbol{s}_q\big), \quad (13)$$

where $\widehat{\{\cdot\}}$ denotes the matrix including kinematic and dynamic parameter errors. The vector, $\widetilde{\boldsymbol{a}} = \boldsymbol{a} - \widehat{\boldsymbol{a}}$, represents the parameter errors, in which $\boldsymbol{a}$ describes a real parameters and $\widehat{\boldsymbol{a}}$ is its estimate. Note that the real parameter vector $\boldsymbol{a}$ is *constant*. $\boldsymbol{\Lambda} \in R^{6\times 6}$ is a positive definite gain matrix in Cartesian space. $\boldsymbol{\Lambda}_q \in R^{n\times n}$ is a positive definite gain matrix in joint space. $\boldsymbol{s}_q$ is a joint space reference error defined as follows:

$$\boldsymbol{s}_q = \dot{\boldsymbol{\phi}}^r - \dot{\boldsymbol{\phi}}. \quad (14)$$

$\widehat{\boldsymbol{H}}_{em}^+ = \widehat{\boldsymbol{H}}_{em}^T\big(\widehat{\boldsymbol{H}}_{em}\widehat{\boldsymbol{H}}_{em}^T\big)^{-1}$ represents the generalized inverse of the coupling matrix $\widehat{\boldsymbol{H}}_{em}$. The above control can be obtained when $\widehat{\boldsymbol{H}}_{em}$ is of full rank. To cope with the singularity problem, damped-least-square (DLS) method is applied in this paper [10]. Yet, solving the singularity problem is still not the main scope of this paper. One who has interest in it should see the references [10] [11] [12].

B. Stability Analysis

The stability of the closed-loop system (6) with the control laws (11), (12), and (13) is analyzed with the following Lyapunov function consisting of the reference kinetic energy error in joint space and the potential energy resulting from the parameter uncertainties.

$$V(t) = \frac{1}{2}\boldsymbol{s}_q^T \boldsymbol{H}^* \boldsymbol{s}_q + \frac{1}{2}\widetilde{\boldsymbol{a}}^T \boldsymbol{\Gamma} \widetilde{\boldsymbol{a}}. \quad (15)$$

The time-derivative of the above Lynapunov function is derived as:

$$\begin{aligned}\dot{V}(t) &= \boldsymbol{s}_q^T\big(\boldsymbol{\tau} - \boldsymbol{H}^*\ddot{\boldsymbol{\phi}}^r - \boldsymbol{c}^*(\boldsymbol{x}_e, \boldsymbol{\eta}, \boldsymbol{\phi}, \dot{\boldsymbol{\phi}}^r)\big) + \widetilde{\boldsymbol{a}}^T\boldsymbol{\Gamma}\dot{\widetilde{\boldsymbol{a}}} \\ &= -\boldsymbol{s}_q^T \boldsymbol{\Lambda}_q \boldsymbol{s}_q \\ &\quad + \boldsymbol{s}_q^T\big(\widehat{\boldsymbol{H}}_{em}^T\dot{\boldsymbol{\eta}} + \widehat{\boldsymbol{H}}\ddot{\boldsymbol{\phi}}^r + \widehat{\boldsymbol{c}}_{em}^T\boldsymbol{\eta} + \widehat{\boldsymbol{c}}_m\dot{\boldsymbol{\phi}}^r - \boldsymbol{H}^*\ddot{\boldsymbol{\phi}} - \boldsymbol{c}^*\big) \\ &\quad + \widetilde{\boldsymbol{a}}^T\boldsymbol{\Gamma}\dot{\widetilde{\boldsymbol{a}}} \\ &= -\boldsymbol{s}_q^T\boldsymbol{\Lambda}_q\boldsymbol{s}_q + \dot{V}_1(t) + \dot{V}_2(t) + \widetilde{\boldsymbol{a}}^T\boldsymbol{\Gamma}\dot{\widetilde{\boldsymbol{a}}}, \end{aligned} \quad (16)$$

where

$$\begin{aligned}\dot{V}_1(t) &= \boldsymbol{s}_q^T\big(\widetilde{\boldsymbol{H}}_{em}^T\dot{\boldsymbol{\eta}} + \widetilde{\boldsymbol{H}}_m\ddot{\boldsymbol{\phi}}^r + \widetilde{\boldsymbol{c}}_{em}^T\boldsymbol{\eta} + \widetilde{\boldsymbol{c}}_m\dot{\boldsymbol{\phi}}^r\big), \\ \dot{V}_2(t) &= \boldsymbol{s}_q^T\boldsymbol{H}_{em}^T\{\dot{\boldsymbol{\eta}} + \boldsymbol{H}_e^{-1}\big(\boldsymbol{H}_{em}\ddot{\boldsymbol{\phi}}^r + \boldsymbol{c}_e\boldsymbol{\eta} + \boldsymbol{c}_{em}\dot{\boldsymbol{\phi}}^r\big)\}.\end{aligned}$$

The term, $\dot{V}_1$, is simply expressed in the linear parameterization form as described in *Property 1*:

$$\dot{V}_1(t) = \boldsymbol{s}_q^T\boldsymbol{Z}\widetilde{\boldsymbol{a}}, \quad (17)$$

where $\boldsymbol{Z} = \boldsymbol{Z}\big(\boldsymbol{x}_e, \boldsymbol{\eta}, \dot{\boldsymbol{\eta}}, \boldsymbol{\phi}, \dot{\boldsymbol{\phi}}^r, \ddot{\boldsymbol{\phi}}^r\big)$.

The term, $\dot{V}_2$, can be also linearly parameterized by using the coordinate mapping from Cartesian space to joint space on the assumption that the constant total linear and angular momentum (*e.g.* $\mathcal{L}_e = \boldsymbol{0}$):

$$\begin{aligned}\dot{V}_2(t) &= \boldsymbol{s}_q^T\boldsymbol{H}_{em}^T\Big\{\dot{\boldsymbol{\eta}} + \boldsymbol{H}_e^{-1}\big(\boldsymbol{H}_{em}\ddot{\boldsymbol{\phi}}^r + \boldsymbol{c}_e\boldsymbol{\eta} + \boldsymbol{c}_{em}\dot{\boldsymbol{\phi}}^r\big)\Big\} \\ &= -\boldsymbol{s}^T\big(\boldsymbol{H}_e\dot{\boldsymbol{\eta}} + \boldsymbol{H}_{em}\ddot{\boldsymbol{\phi}}^r + \boldsymbol{c}_e\boldsymbol{\eta} + \boldsymbol{c}_{em}\dot{\boldsymbol{\phi}}^r\big) \\ &= -\boldsymbol{s}^T\big(\widetilde{\boldsymbol{H}}_e\dot{\boldsymbol{\eta}} + \widetilde{\boldsymbol{H}}_{em}\ddot{\boldsymbol{\phi}}^r + \widetilde{\boldsymbol{c}}_e\boldsymbol{\eta} + \widetilde{\boldsymbol{c}}_{em}\dot{\boldsymbol{\phi}}^r + \boldsymbol{\Lambda}\boldsymbol{s}\big) \\ &= -\boldsymbol{s}^T\boldsymbol{\Lambda}\boldsymbol{s} + \boldsymbol{s}^T\boldsymbol{Y}\widetilde{\boldsymbol{a}}, \end{aligned} \quad (18)$$

where $\boldsymbol{Y} = \boldsymbol{Y}\big(\boldsymbol{x}_e, \boldsymbol{\eta}, \dot{\boldsymbol{\eta}}, \boldsymbol{\phi}, \dot{\boldsymbol{\phi}}^r, \ddot{\boldsymbol{\phi}}^r\big)$.

Consequently, the time-derivative of the Lyapunov function is given as:

$$\begin{aligned}\dot{V}(t) = &-\boldsymbol{s}_q^T\boldsymbol{\Lambda}_q\boldsymbol{s}_q - \boldsymbol{s}\boldsymbol{\Lambda}\boldsymbol{s} \\ &+ \widetilde{\boldsymbol{a}}^T\big(\boldsymbol{Z}^T\boldsymbol{s}_q + \boldsymbol{Y}^T\boldsymbol{s} + \boldsymbol{\Gamma}\dot{\widetilde{\boldsymbol{a}}}\big).\end{aligned} \quad (19)$$

Since the adaptive control law is designed as (13), the above equality results in:

$$\dot{V}(t) = -\boldsymbol{s}_q^T\boldsymbol{\Lambda}_q\boldsymbol{s}_q - \boldsymbol{s}^T\boldsymbol{\Lambda}\boldsymbol{s} \le 0. \quad (20)$$

The control laws (11) and (12) with the parameter update law (13) guarantee the stability and result in the convergence of position and velocity tracking errors of the end-effector in the free-floating space robot, so that $\widetilde{\boldsymbol{x}}_e \to \boldsymbol{0}$ and $\dot{\widetilde{\boldsymbol{x}}}_e \to \boldsymbol{0}$ as $t \to \infty$.

Proof: Since $\boldsymbol{H}^*$ is uniformly positive-definite, V in (15) is positive-definite in $\boldsymbol{s}_q$ and $\widetilde{\boldsymbol{a}}$. Therefore, equation (20) indicates that $V(t) \le V(0)$, and thus $\boldsymbol{s}_q$ and $\widetilde{\boldsymbol{a}}$ are bounded. Equation (5) gives the reference error $\boldsymbol{s}$ as a function of the joint space reference error $\boldsymbol{s}_q$ such that $\boldsymbol{s} = \widetilde{\boldsymbol{J}}_e^*\boldsymbol{s}_q$ where $\widetilde{\boldsymbol{J}}_e^*$ is a function of $\widetilde{\boldsymbol{a}}$. Hence, $\boldsymbol{s}$ is also bounded since $\boldsymbol{s}_q$ and $\widetilde{\boldsymbol{a}}$ are bounded as mentioned above.

Furthermore, the time-derivative of (20) yeilds

$$\ddot{V}(t) = -2\big(\boldsymbol{s}_q^T\boldsymbol{\Lambda}_q\dot{\boldsymbol{s}}_q + \boldsymbol{s}^T\boldsymbol{\Lambda}\dot{\boldsymbol{s}}\big). \quad (21)$$

This indicates that $\ddot{V}$ is bounded since both $\boldsymbol{s}_q$ and $\boldsymbol{s}$ are bounded. Hence, $\dot{V}$ is uniformly continuous. By using Barbalat's lemma, we obtain $\boldsymbol{s}_q \to \boldsymbol{0}$ and $\boldsymbol{s} \to \boldsymbol{0}$ as $t \to \infty$, which leads to $\widetilde{\boldsymbol{x}}_e \to \boldsymbol{0}$ and $\dot{\widetilde{\boldsymbol{x}}}_e \to \boldsymbol{0}$ as $t \to \infty$.△△△

In the implementation of the proposed adaptive controller, sensory feedback of the position and velocity of the end-effector is required as can be seen in (9). However, any acceleration measurement is necessary since the controller is designed by using the feature of dynamical coupling as shown in (11) and (12). Besides, both reference acceleration $\dot{\eta}$ and $\ddot{\boldsymbol{\phi}}^r$ do not involve the acceleration of the system as shown in (9) and (11). Many previous researches have assumed that the acceleration of the Cartesian point is measurable or well-estimated since that assumption allows to simply linearize the parameters in terms of suitable unknown parameters for their adaptive controller design of the free-floating space robot. However, measuring the acceleration on orbit is practically difficult since the measurement is strongly susceptible of a sensor noise and drift. A novel advantage of the proposed adaptive controller in this paper is that it does not involve any measurement of the acceleration; but the system still can be linearized in terms of suitable parameters in adaptive control design as expressed in this section.

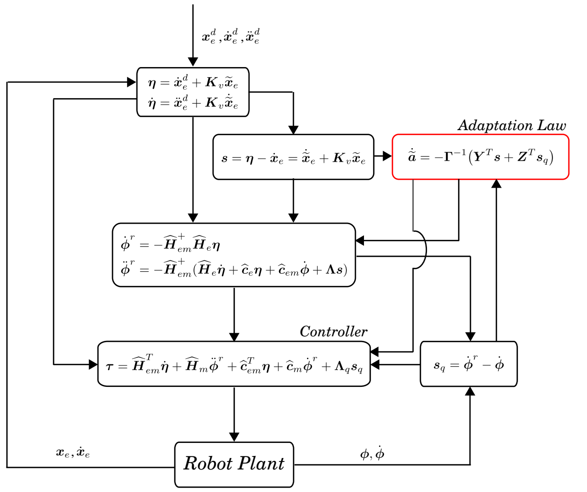

Fig. 3: Control diagram for adaptive trajectory tracking

IV. Simulation Study

The simulation study is carried out to confirm the validity of the proposed adaptive control for a free-floating space robot. In the simulation, the space robot is assumed to track a given trajectory while it firmly grasps a target. The desired trajectory is designed along a circle whose radius is 0.30 [m] and it inclines 30 [deg] about the x axis with respect to the inertial coordinate frame. In the simulation, the initial total linear and angular momentum of the entire system are assumed to be zero. The chaser robot has a seven DOF (R-P-R-P-R-P-P) manipulator system mounted on the base satellite as shown in Fig. 1. The dynamic parameters of the robot are assumed to be well known in advance, as listed in Table II. In the simulation, the target parameters of the planned motion are supposed to be zero, while those of the controlled motion are listed in Table IV. In addition, the parameters of the base satellite of the planned motion are set as listed in Table III, while those of the controlled motion are supposed to be 0.8 times smaller than the parameters listed in Table III. The center of mass of the base satellite and the target in the model are assumed to deviate from those of the real system as listed in Table V and Table VI, respectively. These model errors give the extent of uncertainty introduced in the system. Therefore, the unknown parameter vector $\boldsymbol{a}$ in eq. (13) includes mass, moment of inertia, product of inertia, and center of mass of the base and the target, and then the vector $\boldsymbol{a}$ is expressed by two vectors associated with the base and the target as follows:

$$\boldsymbol{a} = [\boldsymbol{a}_{base}, \boldsymbol{a}_{target}],$$
$$\boldsymbol{a}_i = (m, r_{gx}, r_{gy}, r_{gz}, I_{xx}, I_{yy}, I_{zz}, I_{xy}, I_{yz}, I_{zx},)^T \quad (i = base\ or\ target)$$

TABLE II: Parameters of robot arm

	mass $[kg]$	I_{xx} $[kgm^2]$	I_{yy} $[kgm^2]$	I_{zz} $[kgm^2]$
Link	3.3	0.0056	0.0056	0.0056

TABLE III: Parameters of base satellite

	mass $[kg]$	$I_{xx}[kgm^2]$	$I_{yy}[kgm^2]$	$I_{zz}[kgm^2]$
Base	168	21.6	24.0	26.4

TABLE IV: Parameters of target

	mass $[kg]$	$I_{xx}[kgm^2]$	$I_{yy}[kgm^2]$	$I_{zz}[kgm^2]$
Target	140	18.0	20.0	22.0

TABLE V: Deviation of center of mass of base satellite

	$r_{gx}[m]$	$r_{gy}[m]$	$r_{gz}[m]$
Base	0.05	0.0	0.05

TABLE VI: Deviation of center of mass of target

	$r_{gx}[m]$	$r_{gy}[m]$	$r_{gz}[m]$
Target	0.05	0.0	-0.05

The adaptation gain $\boldsymbol{\Gamma}^{-1}$ in eq. (13) is determined as

$$\boldsymbol{\Gamma}^{-1} = [\boldsymbol{\Gamma}_{base}^{-1}, \boldsymbol{\Gamma}_{target}^{-1}]$$
$$\boldsymbol{\Gamma}_{base}^{-1} = diag(\ [\ 5\times10^2,\ 0.1,\ 0.1,\ 0.1,\ 50,\ 50,\ 50,\ 5\times10^{-4},\ 5\times10^{-4},\ 5\times10^{-4}\ ]).$$
$$\boldsymbol{\Gamma}_{target}^{-1} = diag(\ [\ 1\times10^3,\ 0.1,\ 0.1,\ 0.1,\ 5\times10^3,\ 5\times10^3,\ 5\times10^3,\ 5\times10^{-4},\ 5\times10^{-4},\ 5\times10^{-4}\ ])$$

The control gains $\boldsymbol{K}_v$, $\boldsymbol{\Lambda}$ and $\boldsymbol{\Lambda}_q$ are set

$$\boldsymbol{K}_v = diag([\ 20,\ 20,\ 20,\ 3000,\ 3000,\ 3000\ ]),$$
$$\boldsymbol{\Lambda} = diag([\ 0.3,\ 0.3,\ 0.3,\ 0.3,\ 0.3,\ 0.3\ ]),$$
$$\boldsymbol{\Lambda}_q = diag([\ 0.2,\ 0.2,\ 0.2,\ 0.2,\ 0.2,\ 0.2,\ 0.2\ ].$$

Figure 4 shows the desired and actual trajectories in Cartesian space. In the figure, the red solid line depicts the desired trajectory, the green line depicts the trajectory with parameter deviations but without adaptive control, and the blue line depict the trajectory with adaptive control. Figure 5 shows the trajectory error in the cases with and without adaptive control. The blue solid line depicts the error in the case with adaptive control, while the green dashed line depicts the error in the case without adaptive control. These graphs clearly show that the proposed adaptive control method is effectively used for ensuring trajectory tracking against parameter uncertainties. The representative dynamic parameters, such as mass and moment of inertia about each axis of the base satellite and the target change as shown in Fig. 6. Note that if exact real parameters can be identified, the input command needs to be persistently exciting.

V. Conclusions

This paper proposed an adaptive controller for a torque-controlled fully free-floating space robot with kinematic and dynamic model uncertainty. The proposed method resolved two fundamental difficulties in adaptive control design for the space robots, which are non-linear parameterization in

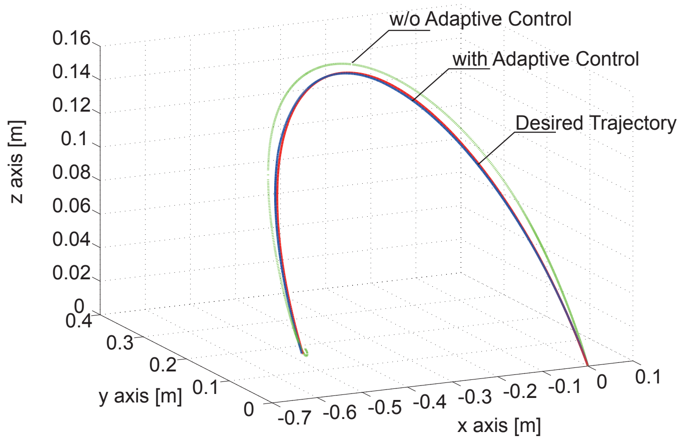

Fig. 4: Trajectory tracking in Cartesian space

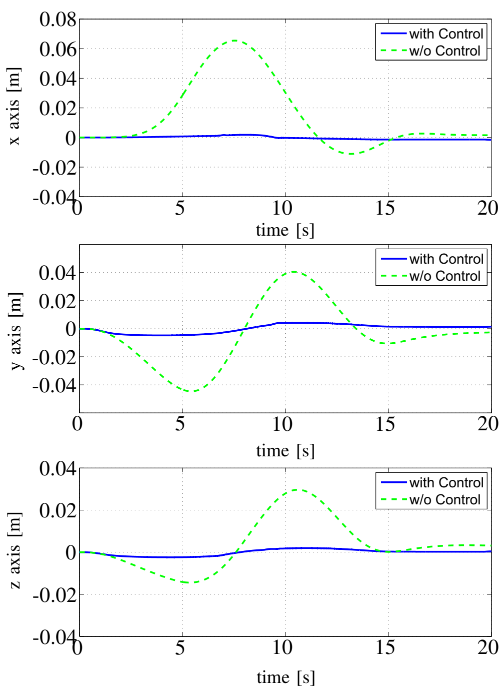

Fig. 5: Trajectory tracking error

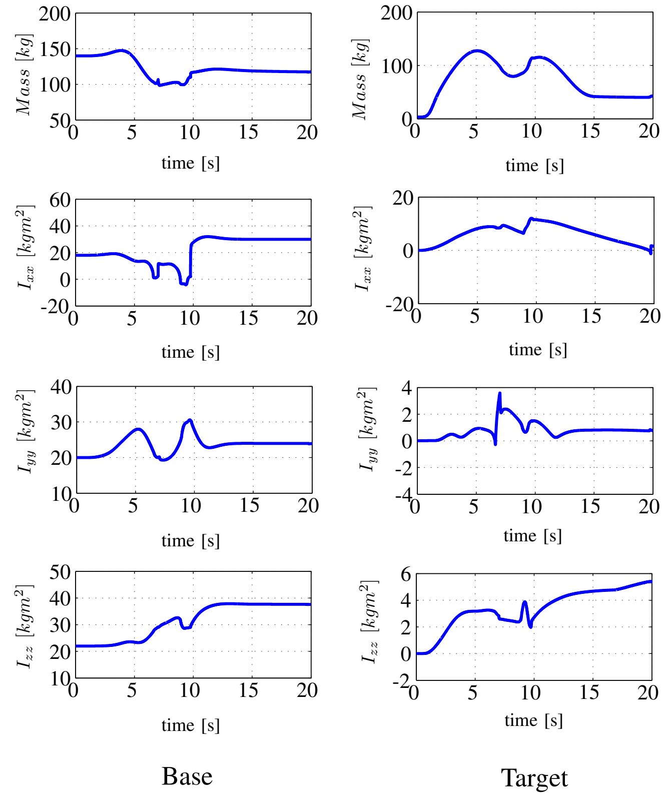

Fig. 6: Adaptation process of the parameters

the dynamic equation and both kinematic and dynamic parameter uncertainties in the coordinate mapping from Cartesian space to joint space. A novel feature of the proposed method is that any acceleration measurement of the Cartesian space is not required; but it is still possible for the system to be linearly parameterized. The results of the simulation demonstrated the efficiency of the proposed adaptive control for the torque controlled free-floating space robot.

References

[1] J. J. E. Slotine and W. Li, “On the Adaptive Control of Robot Manipulators,” *The Int. Journal of Robotics Research*, vol. 6, no. 3, pp. 49 – 59, 1987.

[2] ——, “Adaptive Manipulator Control: A Case Study,” *IEEE Transactions on Automatic Control*, vol. 33, no. 11, pp. 995 – 1003, 1988.

[3] Y. Xu, H.-Y. Shum, J.-J. Lee, and T. Kanade, “Adaptive Control of Space Robot System with an Attitude Controlled Base,” in *Proc. of the 1992 Int. Conf. on Robotics and Automation*, Nice, France, May 1992, pp. 2005 – 2011.

[4] Y. L. Gu and Y. Xu, “A Normal Form Augmentation Approach to Adaptive Control of Space Robot Systems,” in *Proc. of the 1993 IEEE Int. Conf. on Robotics and Automation*, vol. 2, Atlanta, USA, May 1993, pp. 731 – 737.

[5] L.-B. Wee, M. W. Walker, and N. H. McClamroch, “An Articulated-Body Model for a Free-Flying Robot and Its Use for Adaptive Motion Control,” *IEEE Transactions on Robotics and Automation*, vol. 13, no. 2, pp. 264 – 277, April 1997.

[6] S. Abiko and G. Hirzinger, “An Adaptive Control for a Free-Floating Space Robot By Using Inverted Chain Approach,” in *Proc of The 2007 IEEE/RSJ Int. Conf. on Intelligent Robots and Systems*, San Diego, USA, Oct. 2007, pp. 2236 – 2241.

[7] C. C. Cheah, C. Liu, and J. J. E. Slotine, “Adaptive Jacobian Tracking Control of Robots With Uncertainties in Kinematic, Dynamic and Actuator Models,” *IEEE Transactions on Automatic Control*, vol. 51, no. 6, pp. 1024 – 1029, 2006.

[8] Y. Xu and T. Kanade, Eds., *Space Robotics: Dynamics and Control*. Kluwer Academic Publishers, 1993.

[9] Y. Masutani, F. Miyazaki, and S. Arimoto, “Modeling and Sensory Feedback for Space Manipulators,” in *Proc. of the NASA Conf. on Space Telerobotics*, Pasadena, California, USA, Feb. 1989, pp. 287 – 296.

[10] Y. Nakamura and H. Hanafusa, “Inverse Kinematic Solutions with Singularity Robustness for Robot Manipulator Control,” *Journal of Dynamic Systems, Measurement and Control*, vol. 108, pp. 163 – 171, 1986.

[11] S. Chiaverini, “Singularity-Robust Task-Priority Redundancy Resolution for Real-Time Kinematic Control of Robot Manipulators,” *IEEE Trans. on Robotics and Automation*, vol. 13, no. 3, pp. 398 – 410, 1997.

[12] D. N. Nenchev, Y. Tsumaki, and M. Uchiyama, “Singularity-Consistent Parameterization of Robot Motion and Control,” *Int. Journal of Robotics Research*, vol. 19, no. 2, pp. 159 – 182, Feb. 2000.